Journal of Fluorine Chemistry 188 (2016) 126–130

Contents lists available at ScienceDirect

Journal of Fluorine Chemistry

journal homepage: www.elsevier.com/locate/fluor

Short communication

The close interaction of a C—F bond with a carbonyl π–system: Attractive, repulsive, or both?

Maxwell Gargiulo Holl, Mark D. Struble, Maxime A. Siegler, Thomas Lectka*

Department of Chemistry, New Chemistry Building, Johns Hopkins University, 3400 North Charles Street, Baltimore, MD 21218, United States

ARTICLE INFO

Article history:
Received 26 May 2016
Received in revised form 22 June 2016
Accepted 23 June 2016
Available online 24 June 2016

Keywords:
Physical organic
Noncovalent interactions
Electron deformation density

ABSTRACT

We have synthesized a molecule containing a close interaction between a C—F bond and the π–orbitals of a ketone carbonyl group. Our studies have revealed that there is a combination of attractive and repulsive forces at play: the ketone's IR stretching mode is blue-shifted, the carbonyl is bent away from the fluorine atom, and electron deformation density maps show some significant distortion of the fluorine atom's electron density distribution. Finally, binding of the ketone to an aluminum-based Lewis acid deshields the fluorine nucleus. IR and NMR spectroscopy, single crystal X-ray crystallography, and quantum mechanical calculations were used to investigate this unusual interaction.

1. Introduction

Noncovalent interactions are critical to understanding the relationship between chemical structure and reactivity, and can influence events in unusual and initially unpredictable ways. In respect to its noncovalent interactions, fluorine has always been in a class by itself, even when compared to the other halogens. Its small size, high electronegativity, relative lack of polarizability and tendency for monovalency allow it to alter a molecule electronically while having a lesser impact on shape and conformation. One way to understand the properties of these fluorinated molecules is to study their noncovalent interactions with common functional groups [1].

One example of a noncovalent interaction that has been studied extensively is the halogen bond [2,3], which is characterized by the halogen atom serving as a Lewis acid towards a suitable donor [4,5]. This situation creates an electropositive pocket on the halogen, called the "σ–hole," to which the donor is attracted [4]. Halogen bonding interactions are known to affect binding and conformation in the active sites of catalysts [6]. However, due to the small size and high electronegativity of fluorine atoms, its σ–hole is observed in very few cases [7]. However, it is possible that a different type of interaction could produce a structure similar to a σ–hole on a fluorine atom, such as electron-electron repulsion. In this work, we report on compound **1**, which contains a close interaction between fluorine and a ketone C=O π–system. Somewhat similar interactions between a nitrogen atom and a ketone have been previously reported [8]; in the present case, there exists evidence of interactive character between the fluorine and ketone carbonyl, but it differs from that in a halogen bond, but does apparently involve a σ–hole – like region on the fluorine atom. In addition, intermolecular F···C=O short contacts have been observed in crystal packing, but these interactions have not been investigated in depth and differ from the interaction in this work in that in those cases the fluorine atom is unambiguously in contact with only the carbon atom [9]. We have previously synthesized **1** as an intermediate while making other compounds in our previous works [10] (see Supporting information, SI), and only recently recognized that it is an interesting species in its own right; thus it has not been a focus of our investigations until now.

2. Results and discussion

2.1. Molecular geometry

Compound **1** (Fig. 1) prominently features a fluorine atom positioned in proximity and directed towards the keto-carbonyl functional group. The crystal structure of **1** shows short F1–C14 and F1–O4 distances of 2.4417(3) Å and 2.7042(3) Å, respectively (standard uncertainties have been experimentally derived from the MoPro refinements) (Fig. 2). When compared to control **2**, (Fig. 2), the ketone carbonyl is significantly bent away from the fluorine (C1–C14–O4 angle is 114.75°), suggesting that the fluorine's presence has a notable impact on the molecule's overall geometry.

* Corresponding author.
E-mail address: lectka@jhu.edu (T. Lectka).

http://dx.doi.org/10.1016/j.jfluchem.2016.06.016
0022-1139/

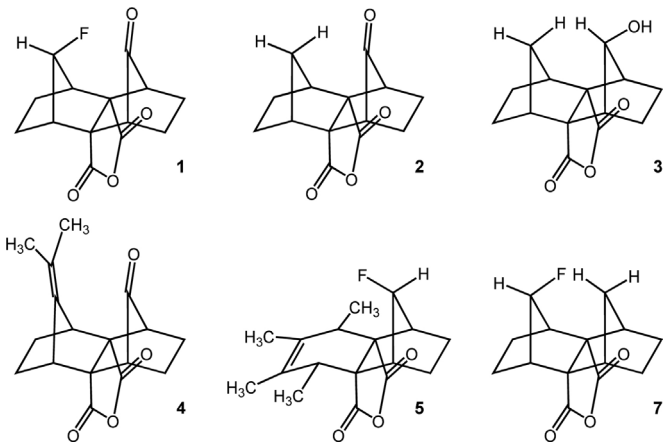

Fig. 1. Compound **1** and various control molecules.

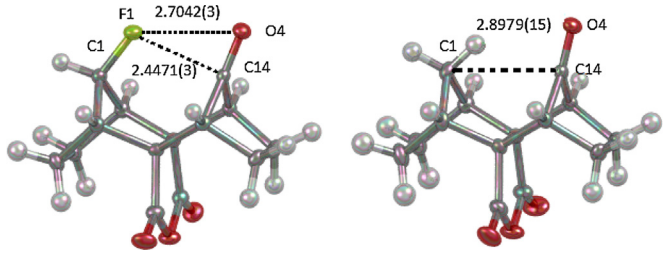

Fig. 2. Displacement ellipsoid plot (50% probability level) of **1** (left) and **2** (right) at 110(2) K. Interatomic distances are given in angstroms.

In a typical halogen bond, the electropositive σ–hole of the halogen coordinates to an electronegative atom. In **1**, the closest electron-rich atom is the ketone oxygen, but the angle about fluorine formed by the C—F bond and ketone oxygen is *ca.* 131°. This is far off from favored 180° "head-on" halogen bond angle, which suggests of course that classical halogen bonding does not occur. Predictably, no obvious evidence for halogen bonding between F and O can be observed in the crystal structure; in contrast to the classical case, the fluorine atom in **1** is aimed at the carbonyl carbon. The tilting of the ketone away from the fluorine atom could also suggest that the F···O interaction may have repulsive character. However, fluorine is most likely presenting an alternate bonding mode between its lone pairs and the electropositive ketone carbon, as a nucleophilic attack frozen in time. This "attack" could also be responsible for the ketone's tilt. Such halogen lone pair–electropositive atom interactions typically have bond angles between 90° and 120°, which fits the 104.6° angle between C1, F1, and C14 [11]. In the ^{13}C NMR spectrum of **1**, the ketone carbon shows a 6.6 Hz coupling to fluorine. This fairly weak coupling suggests that repulsion between the C=O π orbital (which has greater amplitude on oxygen) and fluorine's lone pairs counteracts donation from said lone pairs into the C=O π* antibonding orbital (which has greater amplitude on carbon).

2.2. Infrared spectroscopy

As halogen bonding or any Lewis acid/base pairing affects bond strength, IR spectroscopy should be informative. The C=O stretch of **1** is found at approximately 1785 cm^{-1}, which unfortunately coincides with the analogous anhydride stretches, so we were unable to observe it in isolation. Therefore, to judge the strength of fluorine's perturbation on the ketone properly, a control molecule was needed. As a general statement, one of the greatest difficulties in chemistry is finding appropriate controls for experiments, since to change a part of a system is to change the whole, and observable attributes are generated from multiple interdependent phenomena.

A control was synthesized in the form of **2**, which differs from **1** in that the fluorine is replaced with a hydrogen atom. Alcohol **3** was made as previously reported, and oxidized with PCC to yield **2** (Fig. 1) [12,13]. Its C=O stretching frequency was found at 1762 cm^{-1}. However, it is possible that the *in*-hydrogen in **2** also perturbs the carbonyl. A crystal structure of **2** was obtained that reveals a C1–C14 distance of 2.8979(15) Å (Fig. 2); the two H atoms attached to C1 were placed at calculated positions and refined using a riding model as X-ray crystallography cannot determine them accurately. The C1–C14 distance in **2** is shorter than the C1–C14 distance in **1** (3.1002(4) Å), which indicates that the presence of the fluorine atom in **1** imparts some strain in the molecule. As the cage structure splays open to a greater extent in **1** than in **2** to accommodate the larger fluorine atom, the forced overlap of these groups must be larger, and fluorine should perturb the ketone to a greater extent than the hydrogen.

To gauge the effect the *in*-hydrogen has on the ketone in **2** we decided to employ a second control, with no perturbing atom. Thus we turned to our previously reported olefin **4** (Fig. 1) [14]. Its ketone IR stretch is found at 1764 cm^{-1}, which is 21 cm^{-1} red-shifted compared to **1**. Looking at a calculation of the molecule's vibrational modes at ωB97XD/6-311+G**, it does not appear that its C=O stretch is strongly coupled with the olefin C=C stretch, so it should serve as a good control for an unperturbed ketone in this type of system. As this value is very similar to that of **2** (blue-shifted by only 2 cm^{-1}), it appears that the impact of hydrogen on the C=O stretch is small. Thus, the presence of fluorine is likely the cause of the relative blue shift observed in the C=O stretch of **1**.

2.3. Molecular modeling calculations

Molecular modeling calculations were used to gain a better understanding of the strength of the F···C (carbonyl) interaction. The vibrational modes were computed while fixing the F···C (carbonyl) distances in **1** and the H···C (carbonyl) distances in **2** at values between 2.0 and 3.0 Å (Fig. 3). We chose to run the calculations at the ωB97XD/6-311+G** level of theory, as it has a reputation for correctly predicting dispersion effects [15]. We conducted these calculations using Gaussian 09, and equilibrium molecular coordinates of the structures are available in the SI [16]. The calculated C=O frequency of **1** has its maximum near the fully optimized distance of 2.46 Å. Compound **2** has a maximum frequency at a much greater distance, around 2.7–2.8 Å, while unconstrained optimization gives a distance of 2.28 Å. The blue shift in **1** that occurs on approach from afar can be explained by bond compression, which does not occur in **2**. However, at a certain point, the interaction comes to be dominated by nucleophilic attack of the fluorine on the carbonyl carbon, which red-shifts the C=O stretch; perhaps not coincidentally, the optimized distance lies around the point at which one factor begins to override the other, indicating that both play roles.

2.4. Electron deformation density experiments

We performed an X-ray diffraction experiment at subatomic resolution (maximum resolution at 0.40 Å), and obtained the static deformation electron density map data for **1** (Fig. 4). Initial observations show that the C—F bond seems to have some superficial similarities to a halogen bond. It is evident that there is a large pocket of high electron density on fluorine's side of the C—F bond, and its electron density is being pushed away from the

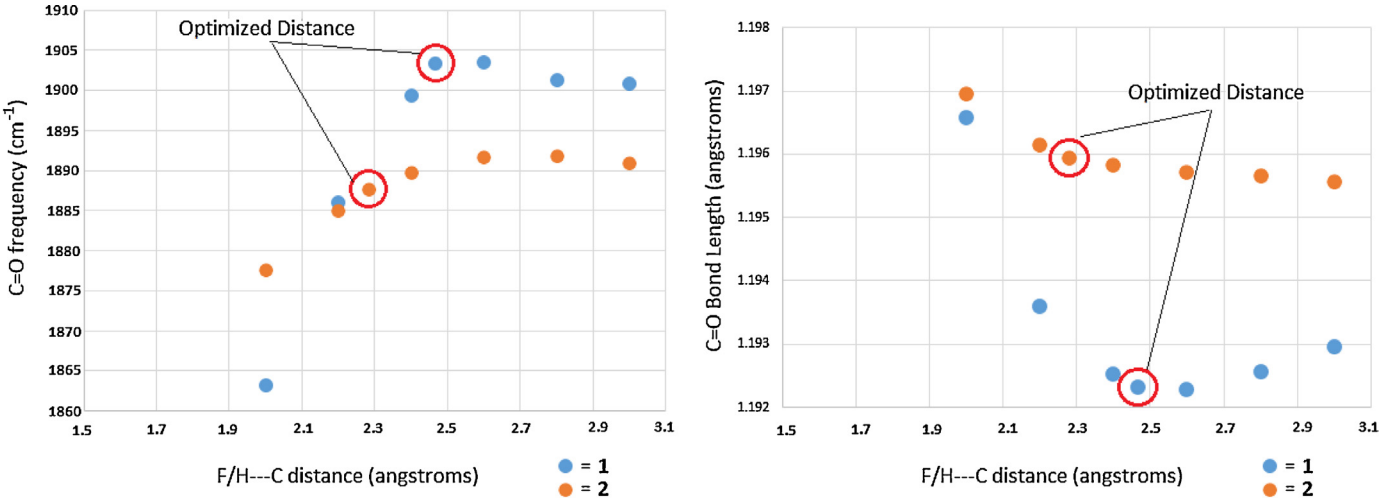

Fig. 3. Plot of C=O frequency and bond length as a function of F···C distance (ωB97XD/6-311+G**).

center of the structure, forming a large lobe near the geminal C—H bond. There are several possible explanations for such interesting behavior. It has been shown that electron-withdrawing groups are able to induce a σ–hole on fluorine through inductive effects [17], and in rare instances through halogen bonding [18]. In addition, there is a large hole present on the carbonyl carbon that points directly at the electron density surrounding the fluorine. This could be evidence for F lone pair ···C=O π* donation. Also, it appears to be typical for fluorine in organic molecules to have a toroidal region of electron density in the plane normal to the C—F bond [19]; the torus is symmetrical (with approximate $D_{\infty h}$ symmetry). In the case of **1**, however, the electron distribution around the F atom is significantly asymmetrical, with more electron density concentrated in the region pointing away from the C=O bond.

The electron density data become more meaningful with proper context, so we again turned to a control molecule. Serendipitously, we synthesized such a species through rather unexpected means. In an attempt to synthesize a molecule with a similar scaffold to **1** with a bridging silicon atom, we observed rapid desilylation and isolated **5** (Fig. 1) instead [20]. The loss of its opposing bridging atom keeps the electron density around the fluorine atom essentially unperturbed. Other minor differences exist between control **5** and **1**, in the form of the four methyl groups and remote double bond, but they are unlikely to act on or be acted upon by electronic perturbations near the fluorine atom. Fig. 4 shows the static deformation electron density map of **5**. One can see that in comparison to **1**, the electron density near fluorine in **5** is more symmetrical, and the hole along the C—F bond is smaller.

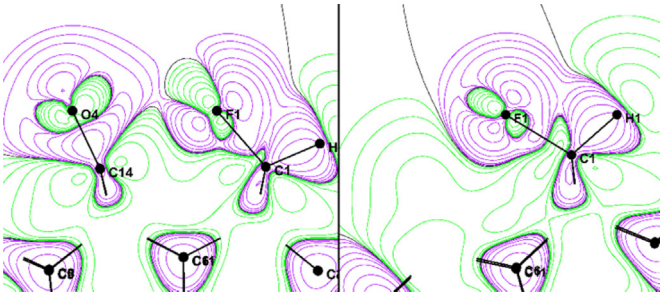

Fig. 4. Static deformation electron density maps of **1** (left) and **5** (right) drawn in the plane H1, C1, F1, 2D slice along the molecule' plane of symmetry. Violet regions represent electron density (positive) and green regions represent holes (negative). (For interpretation of the references to colour in this figure legend, the reader is referred to the web version of this article.)

By comparing the electron density maps of these compounds, some general conclusions can be drawn. Steric effects are often invoked in explaining molecular geometry, usually to explain why certain atoms or groups are rotated or pushed away from each other a la Pauli repulsion. What happens, though, when groups are forced into close contact and the nuclei have very limited range of motion, which prevents relaxation of the system through conformational shifts? It appears that in this case, it is the electrons that move, adopting a new geometric configuration. This is evident in the static deformation electron density map of **1**; whereas some electron density on fluorine is pointed directly at the carbonyl carbon, overall there is less density on the interior side of the fluorine atom and more on the exterior. Thus, electron density flows into this region to the extent that it can be accommodated, but the majority of the density appears on the opposite side as an enlarged electron-rich region. Thus, we gather that when the nuclei are not free to move, the electron cloud ends up in a 'force-fit' situation, where it finds the energetic minimum available to it by balancing an ensemble of attractive and repulsive forces.

Another complementary explanation of some of the observed phenomena, namely the blue shift in the C=O stretch of **1** and the distortion of the electron density near the fluorine atom, is steric compression of both the C—F and C=O bonds, resulting in a bit of bond shortening. The C—F bond in **1** compared to **5** is shorter by 0.00398(21) Å, and the C=O bond in **1** compared to **2** is shorter by 0.0046(16) Å. These values are fairly small, but suggest that steric compression could be partly responsible for our observations. Another observation predicted by steric compression would be deshielding of the ^{19}F nucleus. Indeed, **1** is deshielded compared to **5** by 6.73 ppm. In addition to the static deformation electron density map data, noncovalent interaction (NCI) calculations were performed on **1** using the crystal structure's molecular coordinates (see SI, Fig. S2) [21]. In this case, the calculations show slight attraction between fluorine and the carbonyl carbon, with no apparent interaction between the fluorine and ketone oxygen.

2.5. Lewis acid complex

The inability to observe the ketone stretch of **1** was unfortunate, so we decided to run a final experiment to see if there was some way to reveal it. The use of coordinating Lewis acids to complex with the ketone could perturb the system and shed some light on how it works. Complexation would weaken the carbonyl bond and red-shift it out of the anhydride stretch region. In order to achieve

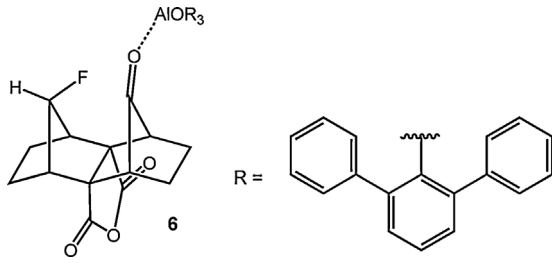

Fig. 5. Putative complex with ATPH.

this, it was necessary to synthesize a Lewis acid that would bind selectively to the ketone and prove that this selectivity was in fact occurring. The first compound that was found to form such a complex successfully was aluminum tris(2,6-diphenylphenoxide) (ATPH) [22]; its coordination to the ketone, forming putative complex **6** (Fig. 5), moved the fluorine atom's chemical shift in ^{19}F NMR from −182.4 to −183.4 ppm. This was accompanied by a new signal in the IR at 1712 cm^{-1}, which we assign to the ketone C=O stretch, red-shifted by its bond with aluminum. Relative *shielding* of the ^{19}F nucleus in the complex compared to **1** is what we would expect to see if steric compression on the C—F bond by the oxygen lone pairs is occurring – as these lone pairs are now involved in a bond to aluminum, their compressive deshielding of the fluorine should be lessened, which is what we observe (by 1 ppm). The Lewis acid was determined to bind selectively to the ketone through rigorous control experiments involving compounds **2** and **7**[12] (Fig. 1), which are detailed as follows. Introducing **1** to 2,6-diphenylphenol resulted in no change in fluorine's chemical shift, indicating that it is indeed the aluminum-based Lewis acid that is binding to the ketone, as opposed to unreacted 2,6-diphenylphenol (which is used in excess). It is possible, but unlikely due to steric effects, that the Lewis acid could bind to the anhydride instead (we selected a very bulky acid to prevent this occurrence). To disprove this possibility we needed a control molecule in which the ketone carbonyl was absent. Fortunately, previously reported compound **7** (Fig. 1) fits these criteria. When this compound was treated with ATPH, there was no observed change in fluorine's chemical shift, nor was there a new signal in the IR spectrum. Therefore, we concluded that the ATPH only binds to the ketone and not the anhydride.

When ATPH was introduced to non-fluorinated control **2**, a new signal at 1712 cm^{-1} was observed in the IR spectrum, indicating that an ATPH-ketone complex similar to **6** had formed. This result rules out the remote, but conceivable, possibility that aluminum is binding directly to fluorine.

3. Conclusions

In conclusion, we demonstrate that **1** manifests an unusual interaction between an organic fluorine atom and a C=O π–system. The observable effects of this interaction are a splaying open of the one-carbon bridges of the molecule's cage structure to distance the fluorine atom from the ketone, a blue shift in the C=O stretch, and a changes in ^{19}F chemical shift and ketone C=O stretch when the ketone is complexed with a Lewis acid. Most revealingly, we observe a strong asymmetrical distribution of the electron density on the fluorine atom, with electron density shifted away from the ketone (save one small region pointed toward the carbonyl carbon), enlarging the apical hole on the fluorine atom. These observations tell the tale of a 'force-fit' situation, where an ensemble of attractive and repulsive forces are at play to accommodate the proximity of the groups, resulting in interesting electronic effects at the interface.

4. Experimental section

4.1. General methods

Unless otherwise stated, all reactions were carried out under strictly anhydrous, air-free conditions under nitrogen. All solvents and reagents were dried and distilled by standard methods. ^{1}H and ^{13}C spectra were acquired on a 400 MHz NMR in $CDCl_3$ at 25 °C; ^{19}F spectra were taken on a 300 MHz NMR in $CDCl_3$ at 25 °C. The ^{1}H, ^{13}C, and ^{19}F chemical shifts are given in parts per million (δ) with respect to an internal tetramethylsilane (TMS, δ 0.00 ppm) standard and/or $CFCl_3$ (δ 0.00 ppm). NMR data are reported in the following format: chemical shifts (multiplicity (s = singlet, d = doublet, t = triplet, q = quartet m = multiplet), integration, coupling constants [Hz]). IR data were obtained using an FT-IR with a flat CaF_2 cell. All measurements were recorded at 25 °C unless otherwise stated. Melting points are uncorrected. Compounds **1**[10], **3**[13], **4**[14], **5**[20], and **7**[12] were prepared according to literature procedures. Spectral and analytical data were in agreement with previous reports. Spectral data were processed with ACD/NMR Processor Academic Edition [23]. Experimental details for theoretical calculations and single crystal X-ray crystallography are presented in the supporting information (SI).

4.2. Compound preparation and characterization

Octahydro-1,4:5,8-dimethano-4a,8a-(methanooxymethano) naphthalene-9,11,12-trione ***(2)***: To a flame dried round-bottom flask equipped with a condenser and large stir bar were added **3** (0.10 g, 0.35 mmol), crushed 3 Å molecular sieves (0.89 g), and potassium carbonate (0.38 g). To the mixture was added DCM (20 mL) followed by cooling to 0 °C. PCC (0.094 g, 0.438 mmol) was added, and the solution was allowed to warm to room temperature before being refluxed overnight. The mixture was then filtered through Celite and concentrated under reduced pressure. The residue was purified by silica gel flash chromatography with a 20% ethyl acetate/hexanes solution to yield **2** as white crystals (0.069 g, 80% yield): mp = 162–165 °C; IR 2963, 2897, 1861, 1780, 1762 (cm^{-1}, CaF_2, CH_2Cl_2); ^{1}H NMR ($CDCl_3$): δ 2.66 (m, 2H), 2.41 (m, 2H), 2.23 (m, 1H), 1.94 (m, 2H), 1.80–1.67, (m, 4H), 1.56 (m, 3H) ^{13}C NMR ($CDCl_3$): δ 209.94, 172.16, 63.60, 44.63, 43.45, 37.85, 26.43, 19.54.

Conflict of interest

The authors declare no competing financial interests.

Acknowledgments

M.D.S. thanks JHU for Gary H. Posner and Rudolph Sonneborn fellowships.

This work was financially supported by the National Science Foundation (NSF CHE-1465131).

We would like to thank JHU for computation time on the MARCC supercomputer.

Appendix A. Supplementary data

Supplementary data associated with this article can be found, in the online version, at http://dx.doi.org/10.1016/j.jfluchem.2016.06.016.

References

[1] K. Müller, C. Faeh, F. Diederich, Science 317 (2007) 1881–1886.

[2] J.P.M. Lommerse, A.J. Stone, R. Taylor, F.J. Allen, J. Am. Chem. Soc. 13 (1996) 3108–3116.
[3] N. Ramasubbu, R. Parthasarathy, P. Murray-Rust, J. Am. Chem. Soc. 15 (1986) 4308–4314.
[4] R. Wilcken, M.O. Zimmermann, A. Lange, A.C. Joerger, F.M. Boeckler, J. Med. Chem. 56 (2013) 1363–1388.
[5] M. Erdélyi, Chem. Soc. Rev. 41 (2012) 3547–3557.
[6] C. Bissantz, B. Kuhn, M. Stahl, J. Med. Chem. 14 (2010) 5061–5084.
[7] P. Metrangolo, J.S. Murray, T. Pilati, P. Politzer, G. Resnati, G. Terraneo, Cryst. Eng. Comm. 22 (2011) 6593–6596.
[8] H.B. Bürgi, J.D. Dunitz, Acc. Chem. Res. 16 (1983) 153–161.
[9] (a) A. Bauzá, A. Terrón, M. Barceló-Oliver, A. García-Raso, A. Frontera, Inorg. Chim. Acta (2015), doi:http://dx.doi.org/10.1016/j.ica.2015.04.028 published online.
[10] M.D. Struble, C. Kelly, M.A. Siegler, T. Lectka, Angew. Chem. Int. Ed. 53 (2014) 8924–8928.
[11] P. Politzer, J.S. Murray, T. Clark, Phys. Chem. Chem. Phys. 28 (2010) 7748–7757.
[12] M.D. Struble, J. Strull, K. Patel, M.A. Siegler, T. Lectka, J. Org. Chem. 79 (2014) 1–6.
[13] M.D. Struble, M.G. Holl, M.T. Scerba, M.A. Siegler, T. Lectka, J. Am. Chem. Soc. 137 (2015) 11476–11490.
[14] M.D. Struble, M.G. Holl, G. Coombs, M.A. Siegler, T. Lectka, J. Org. Chem. 80 (2015) 4803–4807.
[15] (a) J.D. Chai, M. Head-Gordon, Phys. Chem. Chem. Phys. 10 (2008) 6615–6620.
[16] M.J. Frisch, et al., Gaussian 09, Revision A.1, Gaussian Inc., Wallingford, CT, 2009.
[17] (a) P. Metrangolo, J.S. Murray, T. Pilati, P. Politzer, G. Resnati, G. Terraneo, CrystEngComm 13 (2011) 6593–6596.
[18] (a) A.G. Dikundwar, T.N.G. Row, Cryst. Growth Des. 12 (2012) 1713–1716.
[19] M.S. Pavan, K.D. Prasad, T.N.G. Row, Chem. Commun. 49 (2013) 7558–7560.
[20] M.G. Holl, P. Struble, M.A. Siegler, T. Lectka, Angew. Chem. Int. Ed. 128 (2016), doi:http://dx.doi.org/10.1002/ange.201601989 published online.
[21] (a) E.R. Johnson, S. Keinan, P. Mori-Sanchez, J. Contreras-Garcia, A.J. Cohen, W. Yang, J. Am. Chem. Soc. 132 (2010) 6498–6506.
[22] S. Saito, H. Yamamoto, Chem. Commun. 17 (1997) 1585–1592.
[23] ACD/ChemSketch Freeware, Version 12.01, Advanced Chemistry Development, Inc., Toronto, ON, Canada, 2012. www.acdlabs.com.